Transport in Porous Media
https://doi.org/10.1007/s11242-024-02075-y

Magnetic Resonance Relaxation in Heterogeneous Materials is Analogous to First-Order Chemical Reaction

Armin Afrough[1]

Received: 7 November 2023 / Accepted: 13 March 2024

Abstract
Biological tissue, pharmaceutical tablets, wood, porous rocks, catalytic reactors, concrete, and foams are examples of heterogeneous systems that may contain one or several fluid phases. Fluids in such systems carry chemical species that may participate in chemical reactions in the bulk of a fluid, as homogeneous reactions, or at the fluid/fluid or fluid/solid interfaces, as heterogeneous reactions. Magnetic resonance relaxation measures the return of ^{1}H nuclear magnetization in chemical species of these fluids to an equilibrium state in a static magnetic field. Despite the perceived difference between reaction–diffusion and relaxation–diffusion in heterogeneous systems, similarities between the two are remarkable. This work draws a close parallel between magnetic resonance relaxation–diffusion and chemical reaction–diffusion for elementary unitary reaction A → B in a dilute solution—both in heterogeneous systems. A striking similarity between the dimensionless numbers that characterize their relevant behavior is observed: the Damköhler number of the second kind $\mathrm{Da}^{\mathrm{II}}$ for reaction and the Brownstein–Tarr number BT_i for relaxation. The new vision of analogy between reaction- and magnetic resonance relaxation–diffusion in heterogeneous systems encourages the exploitation of similarities between reaction and relaxation processes to noninvasively investigate the dynamics of chemical species and reactions. One such example of importance in chemical engineering is provided for solid–fluid reaction in packed beds.

Keywords Reaction · Diffusion · Relaxation · Magnetic resonance · Analogy · Dimensionless numbers

1 Introduction

A heterogeneous material is composed of domains of different phases. Heterogeneous materials are abundant in nature and technology with examples such as biological tissue, wood, porous rocks, pharmaceutical tablets, catalytic reactors, concrete, and foam (see Fig. 1 for examples). Heterogeneous materials may contain one or several fluid phases.

✉ Armin Afrough
armin@inano.au.dk

[1] Interdisciplinary Nanoscience Center (iNANO), Aarhus University, Gustav Wieds Vej 14, Building 1593, Room 217, 8000 Aarhus C, Denmark

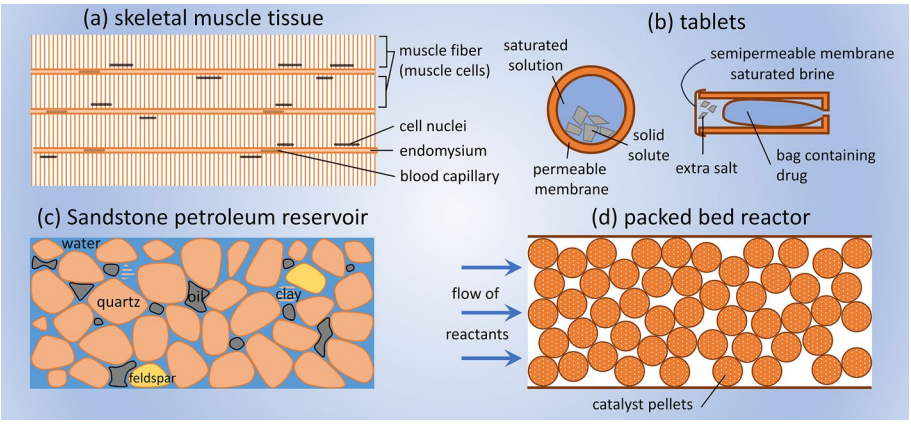

Fig. 1 Examples of fluids in heterogeneous materials with natural and technological origins: **a** skeletal muscle tissue (Schuenke et al. 2006; Rehfeld et al. 2017), **b** pharmaceutical pills with near-zero order release (left) and osmotic pump (right) (Cussler 2009) [pp. 553–556], **c** water and oil in a sandstone petroleum reservoir, and **d** packed bed catalytic reactor

Fluids in such systems carry chemical species that may participate in chemical reactions in the bulk of a fluid, as homogeneous reactions, or at the fluid/fluid or fluid/solid interfaces, as heterogeneous reactions. Water in cytosol and extracellular fluid, blood in artificial kidney, brine and oil in petroleum reservoirs rock pores, moisture in concrete cracks and wood fibers, and methanol production in catalyst pellets are examples of fluids in confinements where physicochemical reactions are prevalent. Fluid phases facilitate transporting chemical species to their reaction site, either in the fluid phase, or at an interface.

Fluid dynamics in heterogeneous materials critically depend on confinements that are key to their function. Geometrical features of confinements sometimes exhibit multiple length scales that challenge predictive modeling of fluid dynamics even when the geometry is known a priori (Kapellos and Alexiou 2013; Holland et al. 2011). Magnetic resonance provides an experimental means of noninvasively probing fluid dynamics in confinements with applicability to a large array of heterogeneous materials through relaxation, diffusion, and imaging (Price 2009).

Magnetic resonance relaxation techniques measure the return of ^{1}H nuclear magnetization that is magnetic moment per unit volume, to its equilibrium condition with a radiofrequency probe in a static magnetic field. In heterogeneous systems, nuclear magnetization relaxes in fluid phases by bulk relaxation and at interfaces by surface relaxation. Fluid and solid interfaces enhance relaxation by homonuclear dipole–dipole coupling, cross relaxation by other nuclear spins, and relaxation by free electrons and paramagnetic ions (Kleinberg 1999). Bulk fluid relaxation mechanisms are the magnetic dipole–dipole interaction, spin rotation, and chemical shift anisotropy among others (Keeler 2010). Despite the perceived difference between reaction–diffusion and relaxation–diffusion in heterogeneous systems, similarities between the two are remarkable.

This work draws a close parallel between dilute first-order A → B chemical reaction–diffusion and magnetic resonance relaxation-diffusion in heterogeneous systems and encourages the development of magnetic resonance methods that exploit this analogy for monitoring chemical reactions and the distribution of chemical species in heterogeneous materials such as biological tissue, artificial organs, catalyst beds, food, and

geological materials. Such new methods have the potential to reveal complex reaction-transport dynamics in opaque materials.

2 Theory

In modeling chemical reactions in bulk or at interfaces, complex underlying mechanisms that are not completely known are reduced to simplified reaction models (Baehr and Stephan 2006) [pp. 234]. In a diffusive conservation of mass partial differential equation, homogeneous reaction appears as a sink term in a volume element and heterogeneous reaction appears as a boundary condition at an interface (Baehr and Stephan 2006) [p. 234].

Consider a single-phase volumetric domain Ω where chemical species A diffuses to an interface $\partial\Omega$ that promotes the first-order irreversible reaction $A \rightarrow B$ and product B diffuses back to bulk fluid—like a solid-catalyzed reaction system (Bird et al. 2002), as shown in Fig. 2a. We make several assumptions that (a) both species A and B are dilute and have similar physical properties, (b) the enthalpy of reaction is zero, and (c) the system is isothermal. The same reaction may also occur homogeneously in the same fluid phase, as shown in Fig. 2b, but at a slower rate

$$R_A(r,t) = k_{\mathrm{HG}} C_A(r,t) \tag{1}$$

at $r \in \Omega$ compared to the heterogeneous reaction with a flux of

$$N_A(r,t) = k_{\mathrm{HT}} C_A(r,t) \tag{2}$$

at the surface $r \in \partial\Omega$ equivalent to the Fourier boundary condition

$$\left(D_A \hat{n} \cdot \nabla + k_{\mathrm{HT}}\right) C_A(r,t) = 0 \tag{3}$$

The geometry of such a 1D system is shown in Fig. 3. Although the reaction is accelerated at the surface, according to Eq. (3), the conversion proceeds at a finite rate because of the diffusion process which is in series with the reaction process.

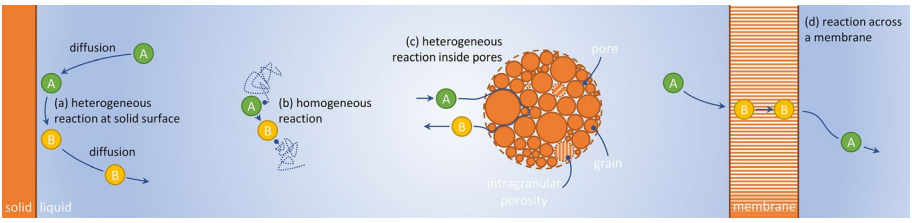

Fig. 2 In heterogeneous systems, reactions and magnetic resonance relaxation may occur **a** at the solid surface, **b** in the bulk fluid, **c** on the interior surface of catalyst, and **d** across a membrane. Examples of such types of chemical reaction and magnetic resonance relaxation are prevalent in nature and technology. In the case of **b** and **c**, reaction and magnetic resonance relaxation may be modeled as if it was homogeneous and characterized by a rate constant. In reactions and magnetic resonance relaxation mediated by surfaces, such as **a** and **d**, diffusion can control reaction and relaxation. See Fig. 16.2–1 in Cussler (2009)

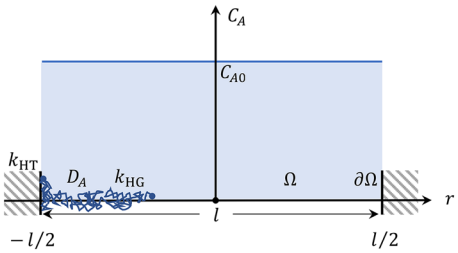

Fig. 3 Homogeneous (with rate constant k_{HG}) and heterogeneous (with rate constant k_{HT}) reactions in a one-dimensional planar geometry with an initial concentration of C_{A0}. Reaction $A \rightarrow B$ may occur in the fluid phase (domain Ω; $r \in (-l/2, l/2)$) or at the surface (domain $\partial\Omega$; $r \in \{-l/2, l/2\}$). The system is in a single dimension, where l is the spacing between pore walls, and the random walk (with diffusivity D_A) of a particle is shown in 2D for demonstration only. Figure 4 demonstrates the evolution of concentration C_A with time

The heterogeneous k_{HT} and homogeneous k_{HG} reaction rate constants quantify the rate of the chemical reaction. Equation (3) serves as the boundary condition to the reaction–diffusion partial differential equation

$$\left(\frac{\partial}{\partial t} - D_A \nabla^2 + k_{HG}\right) C_A = 0 \tag{4}$$

where Equations (3-4) assume a scalar diffusivity D_A. Partial differential Eq. (4), with boundary condition Eq. (3), a given geometry, and an initial condition—such as homogeneous initial concentration $C_A(r, 0) = C_{A0}$—form a complete mathematical system that may be solved to evaluate the concentration evolution $C_A(r, t)$ and chemical amount

$$c_A(t) = \int_\Omega C_A(r, t) dv \tag{5}$$

of species A over time.

In what follows, we demonstrate that a very similar formulation governs magnetic resonance relaxation in heterogeneous systems. Magnetic resonance relaxation methods measure the time-evolution of total nuclear magnetization $m(t)$,

$$m(t) = \int_\Omega M(r, t) dv \tag{6}$$

of ^{1}H nuclei in a sample, where $M(r, t)$ is the magnetic moment per unit volume along some specified direction—M_z parallel to, and M_+ orthogonal to, the static magnetic field. The magnetization evolution $M(r, t)$ during a magnetic resonance experiment in a fluid of self-diffusivity D is governed by the Bloch–Torrey partial differential equation (Torrey 1956)

$$\left(\frac{\partial}{\partial t} - D\nabla^2 + \frac{1}{T_{1b}}\right)\left(M_z - M_0\right) = 0 \tag{7}$$

for longitudinal magnetization M_z and

$$\left(\frac{\partial}{\partial t} - D\nabla^2 + i\gamma G \cdot r + \frac{1}{T_{2b}}\right) M_+ = 0 \tag{8}$$

for transverse magnetization $M_+(r,t)$; T_{1b} and T_{2b} are bulk longitudinal and transverse relaxation time constants, respectively; M_0 is the equilibrium magnetization; D is self-diffusivity.

In heterogeneous domains, magnetization evolution is significantly influenced by fluid interfaces and solid surfaces with the Fourier boundary conditions

$$\left(D\hat{n}\cdot\nabla+\rho_1\right)M_z(r,t)=0 \tag{9}$$

and

$$\left(D\hat{n}\cdot\nabla+\rho_2\right)M_+(r,t)=0 \tag{10}$$

where ρ_1 and ρ_2 are the longitudinal and transverse surface relaxivities, respectively (Brownstein and Tarr 1979). The influence of mechanisms that enhance relaxation at fluid interfaces and solid surfaces are all grouped together only as two surface sink terms ρ_1 and ρ_2. In contrast to surface relaxation, bulk relaxation mechanisms are intrinsic to the fluid phase containing the ^{1}H nuclei and are identified as longitudinal $1/T_{1b}$ and transverse $1/T_{2b}$ relaxation rates. Equations (7–10) together with a geometry and an initial condition—such as homogeneous magnetization $M(r,0)=M_0$—define a mathematical problem that may be solved numerically or, for simple geometries, analytically.

Magnetic field gradient G in Eq. (8) arises from inhomogeneities in the static magnetic field B_0 or internal magnetic field in heterogeneous systems due to the difference between the magnetic susceptibility of phases in the volumetric element under investigation. Internal magnetic field gradients do not affect longitudinal relaxation measurements at all and transverse magnetization relaxation measurements at sufficiently small magnetic field intensities. The effects of magnetic field gradients are therefore neglected in this work.

2.1 Analogy

Magnetic resonance relaxation of ^{1}H nuclei in heterogeneous materials may be formulated as a first-order irreversible reaction

$$\text{Excited}\rightarrow\text{Relaxed}$$

similar to that of the $A\rightarrow B$ chemical reaction. A simple comparison of Eqs. (4) and (7–8), (3) and (9–10), and (5) and (6) readily demonstrates that the relaxation-diffusion problem is analogous to the reaction–diffusion problem in heterogeneous systems. The following terms are analogous:

- Nuclear magnetization $M(r,t)$ and species concentration $C_A(r,t)$,
- Total nuclear magnetization $m(t)$ and chemical amount $c_A(t)$,
- Heterogeneous reaction rate k_{HT} and surface relaxivities ρ_1 and ρ_2,
- Homogeneous reaction rate k_{HG} and bulk relaxation rates $1/T_{1b}$ and $1/T_{2b}$, and
- Diffusivity D_A and self-diffusivity D.

The governing equations and boundary conditions may be transformed to a dimensionless form where the analogy and dimensionless terms emerge. For governing equations—concentration evolution, Eq. (4), and magnetization evolution without magnetic field

gradients, Eq. (8)—quantities are made dimensionless with the characteristic quantities (Bird et al. (2002) [p. 355]) according to

$$\check{r} = \frac{r}{l}, \quad \check{\nabla} = l\,\nabla, \quad \check{\nabla}^2 = l^2\,\nabla^2, \quad \frac{\partial}{\partial \check{t}} = \frac{D}{l^2}\,\frac{\partial}{\partial t}, \quad \check{C}_A = \frac{C_A}{C_{A0}}, \quad \check{M}_+ = \frac{M_+}{M_{+0}}$$

where l is a characteristic length of the geometry, such as bead diameter in a bead pack. In terms of dimensionless variables, Eqs. (4) and (8) take the equivalent forms of

$$\left(\frac{\partial}{\partial \check{t}} - \check{\nabla}^2 + \left[\!\left[\frac{k_{HG}\,l^2}{D_A}\right]\!\right]\right)\check{C}_A = 0 \tag{11}$$

and

$$\left(\frac{\partial}{\partial \check{t}} - \check{\nabla} + \left[\!\left[\frac{l^2}{T_{2b}D}\right]\!\right]\right)\check{M}_+ = 0 \tag{12}$$

where the terms in double brackets are equivalent dimensionless groups. Further dimensionless groups appear in Fourier boundary conditions

$$\left(\hat{n}\cdot\check{\nabla} + \left[\!\left[\frac{k_{HT}\,l}{D_A}\right]\!\right]\right) C_A = 0 \tag{13}$$

and

$$\left(\hat{n}\cdot\check{\nabla} + \left[\!\left[\frac{\rho_2 l}{D}\right]\!\right]\right) M_+ = 0 \tag{14}$$

The only difference would be in the units of nuclear magnetization and species concentration. Nuclear magnetization represents magnetic moment per unit volume, similar to how species concentration represents amount of a species per unit volume. A list of equivalent parameters and their units is shown in Table 1.

Solutions of the reaction–diffusion and relaxation-diffusion problems are similar. In both cases, the solution strongly depends on geometry and the relative contribution of diffusion and reaction/relaxation. This competition is expressed in terms of the Damköhler number of the second kind

Table 1 Equivalency between reaction–diffusion and relaxation-diffusion terms

Description	Chemical reaction Reaction–diffusion	Magnetic resonance relaxation Relaxation–diffusion
Density	$C_A(r,t);[\mathrm{mol/m^3}]$	$M(r,t);[\mathrm{A}/m]$
Amount	$c_A(t);[\mathrm{mol}]$	$m(t);[\mathrm{Am^2}]$
Homogeneous rate constant	$k_{\mathrm{HG}};[1/\mathrm{s}]$	$1/T_{1b}, 1/T_{2b};[1/\mathrm{s}]$
Heterogeneous rate constant	$k_{\mathrm{HT}};[\mathrm{m/s}]$	$\rho_1, \rho_2;[\mathrm{m/s}]$
Diffusivity	$D_A;[\mathrm{m^2/s}]$	$D;[\mathrm{m^2/s}]$

$$\mathrm{Da}^{\mathrm{II}} = \frac{\mathrm{k_{HT}} l}{D_A} \tag{15}$$

for reaction (Bird et al. 2002) [p. 553], and the Brownstein-Tarr number (Afrough et al. 2021)

$$\mathrm{BT}_i = \frac{\rho_i l}{D} \tag{16}$$

for relaxation where l is a characteristic length of the geometry and $i = 1$ or 2 for longitudinal and transverse relaxation. $\mathrm{Da}^{\mathrm{II}}$ describes the effect of surface reaction kinetics on the overall diffusion–reaction process. Large $\mathrm{Da}^{\mathrm{II}}$ implies the existence of concentration gradients within a reaction–diffusion system (Nagy et al. 2012).

The solution to Eqs. (3–5) for $C_A(r,t)$ in a simple one-dimensional planar geometry, as shown in Fig. 3, with a spacing of l and initial concentration of C_{A0} may be expressed as the superposition of orthogonal functions (Brownstein and Tarr 1979; Ye et al. 2022),

$$C_A(r,t) = C_{A0} \sum_n I_n \cos\left(\frac{r}{\sqrt{\tau_n D_A}}\right) e^{-\frac{t}{\tau_n}} \cdot e^{-\frac{t}{k_{\mathrm{HG}}}} \tag{17}$$

where τ_n are from

$$\xi_n = \frac{l/2}{\sqrt{\tau_n D_A}} \tag{18}$$

that are the roots of

$$\xi_n \tan \xi_n = \mathrm{Da}^{\mathrm{II}} \tag{19}$$

and

$$I_n = \frac{4 \sin \xi_n / \xi_n}{2 + \sin\left(2\xi_n\right)/\xi_n} \tag{20}$$

The total amount c_A is

$$c_A(t) = c_{A0} \sum_n J_n e^{-\frac{t}{\tau_n} - \frac{t}{k_{\mathrm{HG}}}} \tag{21}$$

where c_{A0} is the initial amount of species A and

$$J_n = \frac{4 \sin^2 \xi_n}{\xi_n \left(2\xi_n + \sin 2\xi_n\right)} \tag{22}$$

This is assuming that A and B have the same physical properties resulting in no bulk flow in domain Ω. A complete solution of this problem is analogous to the orthogonal function expansion of Brownstein and Tarr (1979) for magnetic resonance relaxation.

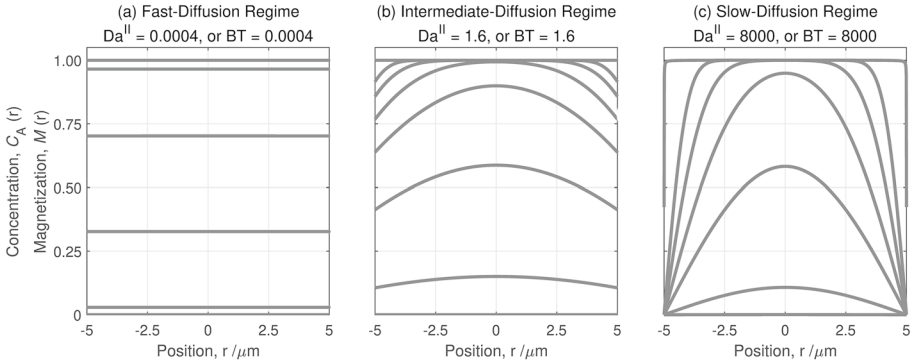

Fig. 4 Concentration $C_A(r)$ (Magnetization $M(r)$) profiles as a function of time evolving by heterogeneous reaction (relaxation) in a one-dimensional planar geometry with an initial concentration of $C_{A0} = 1$ (magnetization of $M_0 = 1$) for **a** fast-diffusion, **b** intermediate-diffusion, and **c** slow-diffusion regimes. Concentration (magnetization) reduces over time due to surface reaction (relaxation) at $r = -5$ and $+5\mu$m. At $\mathrm{Da}^{\mathrm{II}} \to 0$ ($\mathrm{BT} \to 0$) in **a**, diffusion is fast enough to homogenize concentration (magnetization), and at $\mathrm{Da}^{\mathrm{II}} \to \infty$ ($\mathrm{BT} \to \infty$) in (c) reaction (relaxation) is fast enough to maintain a zero concentration (magnetization) at the solid interface

3 Results and Discussion

Figure 4a, b, and c, respectively, demonstrates three example simulations for $\mathrm{Da}^{\mathrm{II}} = 0.0004$, $\mathrm{Da}^{\mathrm{II}} = 1.6$, and $\mathrm{Da}^{\mathrm{II}} = 8000$ (respectively, equivalent to $\mathrm{BT} = 0.0004$, 1.6, and 8000 for magnetic resonance relaxation). In all cases, $D_A = D = 2.5 \times 10^{-9}\mathrm{m}^2/\mathrm{s}$ and $l = 10\mu$m; 1000 simulation points along the r dimension are used with 100 eigenvalues. $k_{\mathrm{HT}} = 0.1$, 400, and $2 \times 10^6 \mu\mathrm{m/s}$ (respectively, equivalent to $\rho = 0.1$, 400, and $2 \times 10^6 \mu\mathrm{m/s}$ for magnetic resonance relaxation) for Fig. 4a, b, and c, respectively. In the extreme case of *reaction-controlled* systems, where $\mathrm{Da}^{\mathrm{II}} \to 0$ similar to that of Fig. 4a, the concentration of substance A in the volumetric domain is uniform. In this case, diffusion is fast enough to homogenize magnetization across the fluid volume. In the other limit of *diffusion-controlled* systems, however, similar to Fig. 4c where $\mathrm{Da}^{\mathrm{II}} \to \infty$, the concentration of substance A at the surface is zero; the diffusion step takes much longer than the reaction step. A realistic physical system however may be far from these two extremes and more similar to that of Fig. 4b.

In magnetic resonance relaxation of sedimentary rocks, it had long been believed that relaxation is in the *fast-diffusion regime* of $\mathrm{BT}_i \to 0$ (Latour et al. 1992), analogous to $\mathrm{Da}^{\mathrm{II}} \to 0$—similar to Fig. 4a. In the limiting case of $\mathrm{BT}_i = 0$, we have $T_{i,0} = l/2\rho_i$ for the ground eigenvalue ($n = 0$), while all nonground eigenvalues $T_{i,n}$ for higher modes ($n > 0$) vanish and may not be observed. Recently, we demonstrated that this conviction is not correct, and BT_i is nonzero and finite for several rock samples (Afrough et al. 2021, 2019). Similar results were observed for glass bead packs and other rock samples as well (Yan et al. 2023). This is similar to the invalidity of the *instantaneous surface reaction* assumption at catalyst surfaces—and close to the case study in the original Brownstein–Tarr work where they concluded a value of $\mathrm{BT}_2 = 4.44$ for the transverse relaxation in rat gastrocnemius muscle (Brownstein and Tarr 1979). In more recent work (Yan et al. 2023), the variation of BT_2 with temperature—between 0.4 to 1.8 in sandstone rocks and glass bead packs—was utilized to determine the absolute pore size from the ground eigenvalue of the relaxation-diffusion equation in simple geometries. It was even possible to observe a

transition between the fast-diffusion regime and diffusion-controlled regime in hydrating cement (Robinson et al. 2023).

In magnetic resonance relaxation experiments, a signal proportional to $m(t)$ measured for a heterogeneous sample may be transformed into the parameters of the relaxation-diffusion system, such as ρ_1 and ρ_2, through parameter-estimation simulations if the geometry is known through complementary imaging methods; for example see (Li et al. 2021, 2022, 2023; Lucas-Oliveira et al. 2020) where X-ray microtomography is employed. Even if the geometry of the system is unknown, eigenvalues of a reduced-physics model may be matched to an exponential analysis of $m(t)$ to evaluate parameters such as the characteristic length l, ρ_1, and ρ_2 by some assumptions; for example see (Yan et al. 2023) for glass bead packs and sandstone, and (Afrough et al. 2019) for bimodal carbonate rock. Such measurements may be performed in bulk, or in the imaging form—spatially resolved (Afrough et al. 2021). In both cases, it is possible to also perform measurements as a function of time inside a magnetic resonance instrument. Since knowledge of the geometry and chemistry of natural and biological systems is often poorly defined, complementary methods and prior information about the sample under study improves the clarity of the physical meaning and uncertainty of quantities acquired by parameter-estimation methods.

3.1 Bulk Relaxation

There are exceptions to the solution presented in the Theory section when the bulk relaxation rate dominates that of surface relaxation—yet with another analogy with chemical reactions in heterogeneous materials. This occurs when diffusion is not fast enough so that all ^{1}H explores the boundaries of confinements (see Fig. 5). This depends on both the extent of the confinement and the nature of fluids. In such examples, protons relax by bulk processes before reaching to the surface of confinements. The Thiele modulus in chemical engineering (Bird et al. 2002) [p. 555]

$$h_T^2 = \frac{k_{\mathrm{HG}} l^2}{D_A} \tag{23}$$

characterizes diffusion with a homogeneous chemical reaction in reaction–diffusion systems which is analogous to the dimensionless number

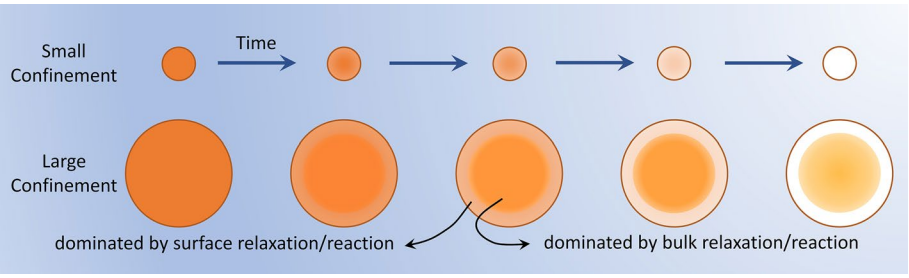

Fig. 5 Evolution of nuclear magnetization in small (top row) and large pores (bottom row) when the bulk relaxation is slower than that of surface relaxation. For magnetic resonance relaxation of ^{1}H, chalk rocks of the North Sea are examples for small confinements (top row) and large vugs in dolostones of the Middle East are examples of large confinements (bottom row). Bulk relaxation, although slower than surface relaxation, eventually completely depletes magnetization in the center of large pores

$$g_i = \frac{l^2}{T_{ib} D} \tag{24}$$

that compares the relative influence of bulk relaxation m/T_{ib} and diffusion mD/l^2. Olaru et al. (2012) had previously called g_i the non-dimensional relaxation time. In large cavities, $g_i \to \infty$ and bulk relaxation dominates, whereas in small confinements $g_i \to 0$ and surface relaxation is dominant. Examples include amniotic fluid surrounding fetus ($g_i > 10^4$) (Saleem 2014), millimeter-sized vugs in dolostones of the Middle East ($g_i > 100$) (Hidajat et al. 2004) and water in small pores of chalk rocks of the North Sea petroleum resources ($g_i < 0.0001$) (Afrough 2021). Relaxation of crude oil in sandstones (Coates et al. 1999), and fluids between large catalyst pellets in packed beds (Weber et al. 2009) are two other notable examples for large g_i. For $g_i \to \infty$, only fluids in the vicinity of the cavity walls will experience surface relaxation; see Fig. 5.

Higher surface reaction and relaxation rates do not mean that homogeneous reaction and bulk relaxation do not contribute to the overall reaction or relaxation. The $1/\tau_n + 1/k_{\mathrm{HG}}$ term in Eq. (21), eigenvalues of the system, demonstrates the contribution of the homogeneous reaction, and in analogy the bulk relaxation. If surface reaction or relaxation is slow enough, it is possible that a large enough number of species A do not experience the reaction or relaxation acceleration. Experimentally, this phenomenon has been observed by the author in longitudinal relaxation of brine in Berea sandstone where a distinct peak for the $1/T_{1b}$ eigenvalue was observed (Afrough et al. 2019). With high signal-to-noise measurement methods (Ardenkjaer-Larsen et al. 2015), therefore, it is possible to measure k_{HG} and T_{ib} in heterogeneous systems where the surface effects are slow enough or large spatial environments exist that are not favorable to surface reaction/relaxation.

3.2 Flow Effects

If in addition to diffusion, there is advection with velocity v, Eq. (4) becomes (Price 2009) [p. 16]

$$\left(\frac{\partial}{\partial t} - D_A \nabla^2 + \nabla \cdot v + k_{HG}\right) C_A = 0 \tag{25}$$

that is analogous to the governing equation for magnetization evolution

$$\left(\frac{\partial}{\partial t} - D\nabla^2 + \nabla \cdot v + \frac{1}{T_{1b}}\right)\left(M_z - M_0\right) = 0 \tag{26}$$

for the longitudinal magnetization and

$$\left(\frac{\partial}{\partial t} - D\nabla^2 + \nabla \cdot v + \frac{1}{T_{2b}}\right) M_+ = 0 \tag{27}$$

for the transverse magnetization. Equations (26–27) are modified Bloch–Torrey equations with flow terms introduced by Stejskal (Stejskal 1965). Equation (27) is correct when there are no internal and external magnetic field gradients. Conditions where, contrary to Eq. (26), external magnetic field gradients are applied are extensively discussed in the magnetic resonance literature.

The governing equations of relaxation-diffusion–advection, Eq. (26), and reaction–diffusion–advection, Eq. (25) are analogous. In fact, the analogy between relaxation-diffusion

and reaction–diffusion displayed in previous sections may be considered as a limiting case where $v \to 0$. Equations (25) and (26) describe a fundamental and scientific description for the concentration and magnetization evolution, respectively. For many realistic conditions, however, these equations may not be accurately solved and matched with experiments. Simpler descriptions for the relaxation of magnetization in complex systems may be adopted from mass transfer coefficients—a concept in chemical engineering.

3.3 Relaxation Time Constants vs. Mass Transfer Coefficients

There are two complementary models which describe mass transfer in science and engineering (Cussler 2009) [p. 333]: description by the (a) diffusion coefficient D_A, and (b) mass transfer coefficient K. The first model describes how the concentration of a species varies with position and time as in Eq. (4) (Cussler 2009) [p. 333]—for example how a drug penetrates human tissue or how excited protons reach surfaces to relax. The second model, however, is used for describing how a chemical species or magnetization is moving from one region into another with flux

$$N_A = K\left(C_{Ai} - C_A\right) \tag{28}$$

that depends on the *well-mixed* bulk concentration C_A, while C_{Ai} is the concentration at the interface (Cussler 2009) [pp. 237–249]. The mass transfer coefficient K with units $\left[\mathrm{m/s}\right]$ is defined per unit interface area.

Mass transfer coefficient is a chemical engineering idea infrequently used in science (Cussler 2009) [p. 334]—at least in its common form. The interfacial area between fluid and solid is not directly measured in many experiments. Instead, the mass transfer rate is expressed as the *volumetric mass transfer coefficient* $Ka = KA/V$ (Cussler 2009) [p. 245], where a is the interfacial surface area A to volume V ratio. Lumping the K and a terms together significantly simplifies the problem and its solution. With this modification, and assuming $C_{Ai} = 0$, the chemical amount is evaluated as (Cussler 2009) [pp. 241–242]

$$c_A(t) = c_{A0} e^{-\frac{KA}{V}t} \tag{29}$$

which has the familiar exponential form corresponding to the fast-diffusion regime with Ka equivalent to $2\rho/l$ in relaxation-diffusion and $2k_{HT}/l$ for reaction–diffusion in the planar geometry. In reality however, the volumetric mass transfer coefficient depends on fluid properties, surface properties, fluid dynamics, and surface geometry. Equation (29) is derived for the 1D problem with $C_{Ai} = 0$ and flux Eq. (28). In heterogeneous materials, the volumetric mass transfer coefficient Ka and magnetic resonance relaxation rate $1/T_i$ terms are analogous – where $i = 1$ or 2 for longitudinal and transverse relaxation, respectively. In fact, relaxation time constants T_i used in radiology (Quantitative MRI of the Brain 2018) are also analogous to $1/Ka$ term (where $a = A/V$) that is a fixture of many mass transfer correlations in chemical engineering (Cussler 2009) [p. 242].

We can decide which aspects of the physical chemistry to ignore and choose the type of description leading to the simplest results (Cussler 2009) [p. 455]. It may be possible to use both Eqs. (21) and (29) to model *dominant* features of magnetic resonance relaxation in porous materials—see (Lucas-Oliveira et al. 2021) for a comparison between the two models in sandstones. Sometimes whether chemical reaction or magnetic resonance relaxation is heterogeneous or homogeneous is a question of judgment (Cussler 2009) [p. 455]. For example, it may be easier to model clay agglomerates in sandstones (that are

similar to Fig. 2c, see also Fig. 1c) as homogeneous systems due to their complex geometry. This is despite the fact that they are actually heterogeneous domains (Cussler 2009) [pp. 456–457]. In some cases, it may be easier to even develop computational systems that use both of these concepts. For example, Li et al. (Li et al. 2021) employed a homogeneous magnetic resonance relaxation rate for describing the behavior of clay agglomerates, which are similar to Fig. 1c, embedded in a porous system with well-defined pore walls, similar to Fig. 1a

3.4 Applying Relaxation Analogy to Mass Transfer in Packed Beds

The analogy between mass-, heat-, and momentum-transfer is a widely used analogy in chemical engineering. This analogy permits obtaining binary mass transfer coefficients at low-mass transfer rates directly from their heat transfer analogs—simply by a change of notation (Bird et al. 2002) [p. 679]. In a similar manner, we harness the similarity between relaxation and reaction in heterogeneous materials and use the analogy developed between the relaxation rate in confinements $1/T_i$ and the volumetric mass transfer coefficient Ka in packed beds.

Fluid–solid mass transfer in packed beds (see Fig. 1d for the representation of a packed bed) has been investigated by a variety of methods (Wakao and Funazkri 1978) in simplified physical models—with model pellets and fluids. Such experimental results (see Fig. 6, gray markers and correlation line) are usually expressed in dimensionless Reynolds $\mathrm{Re} = \rho v l/\mu$,

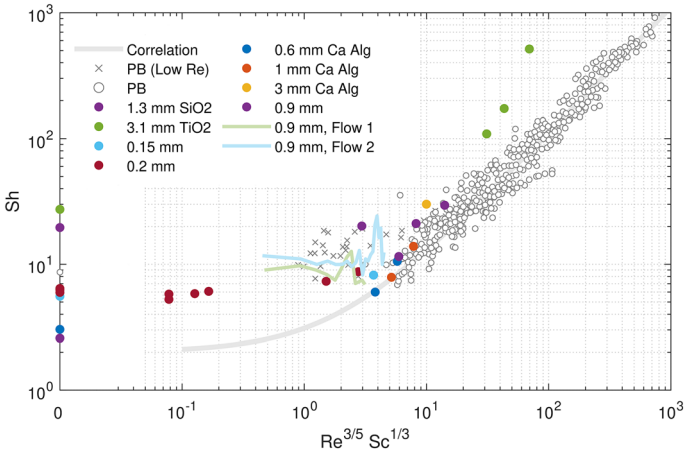

Fig. 6 Correlation between dimensionless Sherwood Sh, Reynolds Re, and Schmidt Sc numbers in packed beds (PB); Data have the same trend for both of chemical engineering experiments (∘, ×) and reaction-relaxation analogy (colored circles). Sherwood number from reaction-relaxation analogy is calculated from $\mathrm{Sh} = l/aT_{2,0}D$ where $1/T_{2,0}$ is the ground eigenvalue of relaxation-diffusion equation with removing bulk relaxation effects for bead packs. Surface area to volume ratio for bead packs is $a = 6(1-\phi)/\phi l$ where ϕ is porosity and l is bead diameter. Sherwood number $\mathrm{Sh} = Kl/D$ in chemical engineering is usually employed in designing packed beds for calculating the solid–fluid mass transfer coefficient K; $\mathrm{Re} = \rho v l/\mu$, and $\mathrm{Sc} = \mu/\rho D$. Both data groups are consistent with the correlation $\mathrm{Sh} = 2 + 1.1\mathrm{Re}^{3/5}\mathrm{Sc}^{1/3}$ (grey line) Chemical engineering data (gray circles) are from (Wakao and Funazkri 1978; Elgersma et al. 2022; Miyauchi et al. 1976; Seguin et al. 1996). Experimental data for magnetic resonance relaxation data are from (Olaru et al. 2012; Britton et al. 2004, 2001; Scheven et al. 2004; Elgersma et al. 2022; Mitchell et al. 2008) and closely match the trend of chemical engineering data. Two colored lines (blue and green) are from 2D displacement-relaxation correlation experiments (Britton et al. 2004). Static data are shown at 0 in the horizontal axis. See supplementary materials for a list of data points

Schmidt $\mathrm{Sc} = \mu/\rho D$, Péclet $\mathrm{Pe} = vl/D$, and Sherwood $\mathrm{Sh} = Kl/D$ numbers; where ρ is density, μ is viscosity, v is fluid velocity, and K is the mass transfer coefficient. Later, correlations from dimensionless numbers are used to calculate parameters of interest in engineering design and analysis. The correlation (Wakao and Funazkri 1978)

$$\mathrm{Sh} = 2 + 1.1\mathrm{Re}^{3/5}\mathrm{Sc}^{1/3} \tag{30}$$

is developed from an extensive experimental dataset and is one such equation that has been extensively used in chemical engineering design for calculating K in packed beds.

Equation (30) is relevant to the reaction–diffusion–advection process in packed beds—with no apparent connection to magnetic resonance relaxation. The analogy discussed in previous sections, however, demonstrates that magnetic resonance relaxation in packed beds of glass beads follow a similar behavior when the Sherwood number is evaluated from magnetic resonance parameters: $\mathrm{Sh}_{\mathrm{MR}} = l/aT_iD$.

Figure 6 demonstrates the correlation between $\mathrm{Sh}_{\mathrm{MR}}$ and $\mathrm{Re}^{3/5}\mathrm{Sc}^{1/3}$ in color *solely from magnetic resonance relaxation-reaction analogy* and Sh in gray from chemical engineering measurements of Wakao and Funazkri (1978); Elgersma et al. (2022), Miyauchi et al. (1976), and Seguin et al. (1996). Magnetic resonance relaxation data are acquired from the literature of T_2 for bead packs as a function of fluid velocity (Olaru et al. 2012; Britton et al. 2004, 2001; Scheven et al. 2004; Elgersma et al. 2022). Figure 6 shows $\mathrm{Sh}_{\mathrm{MR}} = l/aT_iD$ —from the analogy between Ka and $1/T_i$—as a function of $\mathrm{Re}^{3/5}\mathrm{Sc}^{1/3}$ where T_i is the ground eigenvalue of magnetic resonance relaxation. Data collected include glass (Olaru et al. 2012; Britton et al. 2001), alginate (Britton et al. 2004), porous silica (Elgersma et al. 2022), porous anatase titania (Elgersma et al. 2022), and porous glass (Scheven et al. 2004) bead packs. A close similarity between the chemical engineering data (gray markers) (Wakao and Funazkri 1978; Miyauchi et al. 1976; Seguin et al. 1996), chemical engineering correlation of Eq. (30) (solid gray line), and magnetic resonance relaxation data (colored markers) is observed across several orders of magnitude. Two colored lines are from the distance-relaxation correlation experiments (Britton et al. 2004). Magnetic resonance relaxation can extend the correlation to very low Pe numbers. Bias to larger values of Sherwood numbers for porous anatase titania (Elgersma et al. 2022) is likely to be due to the transverse relaxation parameter affected by diffusion in the internal magnetic field gradients (at 7 T). Assumptions were made for the bulk fluid relaxation time constants (with data from Afrough et al. (2021)), the interfacial surface to area $a = 6(1-\phi)/\phi l$ for random close packs (Davies et al. 2007), the experiment temperature (25 °C), and the bed porosity (porosity $\phi = 0.38$) that were absent in some of these studies. A good correlation with the model is observed in three orders of magnitude of $\mathrm{Re}^{3/5}\mathrm{Sc}^{1/3}$. Elgersma et al. (2022) have previously used this correlation and demonstrated that they can measure mass transfer in a packed bed by the transverse relaxation correlation $\left(T_2 - T_2\right)$ magnetic resonance experiments without the analogy demonstrated here. Their data are presented in Fig. 6.

3.5 Perspective

In complex natural and industrial systems, such as living organisms (Kapellos and Alexiou 2013; Holland et al. 2011) and reactors (Ge et al. 2019), the internal dynamics of reaction–diffusion systems is very complex and cannot be readily characterized or modeled especially due to the existence of multiple environments, and length and time scales.

Quantitative magnetic resonance relaxation provides a vision into the internal diffusion dynamics of such systems with negligibly perturbing diffusing molecules.

Although magnetic resonance relaxation may seem to be dominated by surface relaxation and not have any chemical specificity, rotational or translational diffusion may be able to identify the dynamics of distinct chemicals or chemical groups in heterogeneous environments (Leutzsch et al. 2019; Robinson et al. 2021). Multidimensional chemical shift magnetic resonance measurement and analysis methods have also been shown to be capable of providing this chemical specificity without considering the diffusion dynamics (Terenzi et al. 2019). Therefore, at least in model systems, it should be possible to obtain indications of fluid dynamics of distinct molecular species in heterogeneous systems.

The new vision of analogy between reaction- and magnetic resonance relaxation-diffusion in heterogeneous systems encourages the exploitation of similarities between reaction and relaxation processes for noninvasively investigating the dynamics of chemical species and reactions in biological tissue, catalysis, and the environment. Recently, the reaction-relaxation similarity has been used in magnetic resonance of porous media (Afrough et al. 2021, 2019; Maneval et al. 2019) and hyperpolarization transfer to solids (Prisco et al. 2021; Prisco 2020). The accuracy of data in natural systems is often uncertain because of wide variations. It is however possible to inspect experimental results to find natural phenomena and mechanisms that are consistent with these experimental results. The new vision formed by the analogy also makes magnetic resonance relaxation more accessible to non-experts.

Combining magnetic resonance relaxation monitoring and simplified-physics models in heterogeneous materials can advance our understanding of combined reaction-relaxation systems. We anticipate the development of multidimensional magnetic resonance methods and complementary models that characterize the interaction of individual chemical species with the microstructures as well as their chemical reactions in the future. Two example reaction systems are suggested that can potentially demonstrate both reaction and diffusion dynamics: (1) catalytic hydrogenation of alkenes (Leutzsch et al. 2019) and (2) deuteration of organic compounds (Sawama et al. 2019). Both experiments may be performed in NMR tubes (Leutzsch et al. 2019) at near room temperature and exhibit reactions in the presence of catalyst pellets or powders. Chemical reactions and dynamics would both affect the ground eigenvalues of magnetic resonance relaxation in such systems while more accurate information about fluid dynamics may be acquired from comparing relaxation time constants T_1 and T_2 as well as quantitatively analyzing their nonground eigenvalues.

Supplementary Information The online version contains supplementary material available at https://doi.org/10.1007/s11242-024-02075-y.

Acknowledgements The author would like to thank Dr. Martin D. Hürlimann, Profs. Mladen Eić and Laura Romero-Zerón, and especially Profs. Thomas Vosegaard and Bruce J. Balcom for discussions and comments.

Author Contributions The author is responsible for conceptualization, analysis, writing.

Funding Open access funding provided by Aarhus Universitet. The author declares that no funds, grants, or other support were received during the preparation of this manuscript.

Data Availability The dataset used in Fig. 6 is available as supplementary material.

Declarations

Conflict of interest The author has no relevant financial or non-financial interests to disclose.

References

Afrough, A.: Magnetic resonance free induction decay in geological porous materials. Eur. Phys. J. E **44**, 107 (2021). https://doi.org/10.1140/epje/s10189-021-00110-0

Afrough, A., Vashaee, S., Romero Zerón, L., Balcom, B.: Absolute measurement of pore size based on non-ground eigenstates in magnetic-resonance relaxation. Phys. Rev. Appl. **11**, 041002 (2019). https://doi.org/10.1103/PhysRevApplied.11.041002

Afrough, A., Marica, F., MacMillan, B., Balcom, B.J.: Pore-size measurement from eigenvalues of magnetic resonance relaxation. Phys. Rev. Appl. **16**, 034040 (2021). https://doi.org/10.1103/PhysRevApplied.16.034040

Ardenkjaer-Larsen, J.-H., Boebinger, G.S., Comment, A., Duckett, S., Edison, A.S., Engelke, F., Griesinger, C., Griffin, R.G., Hilty, C., Maeda, H., Parigi, G., Prisner, T., Ravera, E., van Bentum, J., Vega, S., Webb, A., Luchinat, C., Schwalbe, H., Frydman, L.: Facing and overcoming sensitivity challenges in biomolecular NMR spectroscopy. Angew. Chemie Int. Ed. **54**, 9162–9185 (2015). https://doi.org/10.1002/anie.201410653

Baehr, H.D., Stephan, K.: Heat and mass transfer, Springer Berlin Heidelberg, Berlin, Heidelberg, (2006). https://doi.org/10.1007/3-540-29527-5

Bird, R.B., Stewart, W.E., Lightfoot, E.N.: Transport phenomena, 2nd edn. Wiley, New York (2002)

Britton, M.M., Graham, R.G., Packer, K.J.: Relationships between flow and NMR relaxation of fluids in porous solids. Magn. Reson. Imaging **19**, 325–331 (2001). https://doi.org/10.1016/S0730-725X(01)00244-2

Britton, M.M., Graham, R.G., Packer, K.J.: NMR relaxation and pulsed field gradient study of alginate bead porous media. J. Magn. Reson. **169**, 203–214 (2004). https://doi.org/10.1016/j.jmr.2004.04.016

Brownstein, K.R., Tarr, C.E.: Importance of classical diffusion in NMR studies of water in biological cells. Phys. Rev. A **19**, 2446–2453 (1979). https://doi.org/10.1103/PhysRevA.19.2446

Coates, G.R., Xiao, L., Prammer, M.G.: NMR logging: principles and applications, halliburton energy services, Houston, (1999)

Cussler, E.L.: Diffusion: mass transfer in fluid systems, Third Edition, 3rd edn. Cambridge University Press, New York (2009)

Davies, C.J., Griffith, J.D., Sederman, A.J., Gladden, L.F., Johns, M.L.: Rapid surface-to-volume ratio and tortuosity measurement using Difftrain. J. Magn. Reson. **187**, 170–175 (2007). https://doi.org/10.1016/j.jmr.2007.04.006

Elgersma, S.V., Sederman, A.J., Mantle, M.D., Gladden, L.F.: Measuring the liquid-solid mass transfer coefficient in packed beds using T2–T2 relaxation exchange NMR. Chem. Eng. Sci. **248**, 117229 (2022). https://doi.org/10.1016/j.ces.2021.117229

Ge, W., Chang, Q., Li, C., Wang, J.: Multiscale structures in particle–fluid systems: characterization, modeling, and simulation. Chem. Eng. Sci. **198**, 198–223 (2019). https://doi.org/10.1016/j.ces.2018.12.037

Hidajat, I., Mohanty, K.K., Flaum, M., Hirasaki, G.: Study of Vuggy carbonates using NMR and x-ray CT scanning. SPE Reserv. Eval. Eng. **7**, 365–377 (2004). https://doi.org/10.2118/88995-PA

Holland, E.C., Watton, P.N., Ventikos, Y.: Biological fluid mechanics. Compr. Biotechnol. (2011). https://doi.org/10.1016/B978-0-08-088504-9.00529-8

Kapellos, G.E., Alexiou, T.S.: Modeling momentum and mass transport in cellular biological media: from the molecular to the tissue scale. Transp. Biol. Media (2013). https://doi.org/10.1016/B978-0-12-415824-5.00001-1

Keeler, J.: Understanding NMR spectroscopy, Wiley, (2010)

Kleinberg, R.L.: Nuclear magnetic resonance, In: P. Wong (Ed.), Methods Phys. Porous Media, Vol. 35, Academic Press, San Diego, 1999: pp. 337–385. https://doi.org/10.1016/S0076-695X(08)60420-2

Latour, L., Kleinberg, R., Sezginer, A.: Nuclear magnetic resonance properties of rocks at elevated temperatures. J. Colloid Interface Sci. **150**, 535–548 (1992). https://doi.org/10.1016/0021-9797(92)90222-8

Leutzsch, M., Sederman, A.J., Gladden, L.F., Mantle, M.D.: In situ reaction monitoring in heterogeneous catalysts by a benchtop NMR spectrometer. Magn. Reson. Imaging **56**, 138–143 (2019). https://doi.org/10.1016/j.mri.2018.09.006

Li, R., Shikhov, I., Arns, C.H.: Solving multiphysics, multiparameter, multimodal inverse problems: an application to nmr relaxation in porous media. Phys. Rev. Appl. **15**, 054003 (2021). https://doi.org/10.1103/PhysRevApplied.15.054003

Li, R., Shikhov, I., Arns, C.H.: Bayesian optimization with transfer learning: a study on spatial variability of rock properties using NMR relaxometry. Water Resour. Res. (2022). https://doi.org/10.1029/2021WR031590

Li, R., Shikhov, I., Arns, C.: A Bayesian optimization approach to the simultaneous extraction of intrinsic physical parameters from T 1 and T 2 relaxation responses. SPE J. **28**, 319–341 (2023). https://doi.org/10.2118/210563-PA

Lucas-Oliveira, E., Araujo-Ferreira, A.G., Trevizan, W.A., dos Santos, B.C.C., Bonagamba, T.J.: Sandstone surface relaxivity determined by NMR T2 distribution and digital rock simulation for permeability evaluation. J. Pet. Sci. Eng. **193**, 107400 (2020). https://doi.org/10.1016/j.petrol.2020.107400

Lucas-Oliveira, E., Araújo-Ferreira, A.G., Bonagamba, T.J.: Surface relaxivity probed by short-diffusion time NMR and digital rock NMR simulation. J. Pet. Sci. Eng. **207**, 109078 (2021). https://doi.org/10.1016/j.petrol.2021.109078

Maneval, J.E., Nelson, M.L., Thrane, L.W., Codd, S.L., Seymour, J.D.: A two-region transport model for interpreting T1–T2 measurements in complex systems. J. Magn. Reson. **308**, 106592 (2019). https://doi.org/10.1016/j.jmr.2019.106592

Mitchell, J., Graf von der Schulenburg, D.A., Holland, D.J., Fordham, E.J., Johns, M.L., Gladden, L.F.: Determining NMR flow propagator moments in porous rocks without the influence of relaxation. J. Magn. Reson. **193**, 218–225 (2008). https://doi.org/10.1016/j.jmr.2008.05.001

Miyauchi, T., Kataoka, H., Kikuchi, T.: Gas film coefficient of mass transfer in low Péclet number region for sphere packed beds. Chem. Eng. Sci. **31**, 9–13 (1976). https://doi.org/10.1016/0009-2509(76)85002-6

Nagy, K.D., Shen, B., Jamison, T.F., Jensen, K.F.: Mixing and dispersion in small-scale flow systems. Org. Process Res. Dev. **16**, 976–981 (2012). https://doi.org/10.1021/op200349f

Olaru, A.M., Kowalski, J., Sethi, V., Blümich, B.: Exchange relaxometry of flow at small Péclet numbers in a glass bead pack. J. Magn. Reson. **220**, 32–44 (2012). https://doi.org/10.1016/j.jmr.2012.04.015

Price, W.S.: NMR studies of translational motion, Cambridge University Press, Cambridge, 2009. https://doi.org/10.1017/CBO9780511770487

Prisco, N.A.: Correlated structure-property relationships in cementitious solids via unconventional spin polarization transfer. University of California, Santa Barbara (2020)

Prisco, N.A., Pinon, A.C., Emsley, L., Chmelka, B.F.: Scaling analyses for hyperpolarization transfer across a spin-diffusion barrier and into bulk solid media. Phys. Chem. Chem. Phys. **23**, 1006–1020 (2021). https://doi.org/10.1039/D0CP03195J

Quantitative MRI of the Brain: CRC Press (2018). https://doi.org/10.1201/b21837

Rehfeld, A., Nylander, M., Karnov, K.: Compendium of Histology, Springer International Publishing, Cham, 2017. https://doi.org/10.1007/978-3-319-41873-5

Robinson, N., May, E.F., Johns, M.L.: Low-field functional group resolved nuclear spin relaxation in mesoporous silica. ACS Appl. Mater. Interfaces **13**, 54476–54485 (2021). https://doi.org/10.1021/acsami.1c13934

Robinson, N., Nasharuddin, R., Fridjonsson, E.O., Johns, M.L.: NMR surface relaxivity in a time-dependent porous system. Phys. Rev. Lett. **130**, 126204 (2023). https://doi.org/10.1103/PhysRevLett.130.126204

Saleem, S.N.: Fetal MRI: an approach to practice: a review. J. Adv. Res. **5**, 507–523 (2014). https://doi.org/10.1016/j.jare.2013.06.001

Sawama, Y., Nakano, A., Matsuda, T., Kawajiri, T., Yamada, T., Sajiki, H.: H-D exchange deuteration of arenes at room temperature. Org. Process Res. Dev. **23**, 648–653 (2019). https://doi.org/10.1021/acs.oprd.8b00383

Scheven, U.M., Seland, J.G., Cory, D.G.: NMR propagator measurements on flow through a random pack of porous glass beads and how they are affected by dispersion, relaxation, and internal field inhomogeneities. Phys. Rev. E **69**, 021201 (2004). https://doi.org/10.1103/PhysRevE.69.021201

Schuenke, M., Schulte, E., Schumacher, U., Rude, J.: Atlas of anatomy: general anatomy and musculoskeletal system. Thieme, Stuttgart (2006)

Seguin, D., Montillet, A., Brunjail, D., Comiti, J.: Liquid—solid mass transfer in packed beds of variously shaped particles at low Reynolds numbers: experiments and model. Chem. Eng. J. Biochem. Eng. J. **63**, 1–9 (1996). https://doi.org/10.1016/0923-0467(96)03073-4

Stejskal, E.O.: Use of sping echoes in a pulsed magnetic-field gradient to study anisotropic, restricted diffusion and flow. J. Chem. Phys. **43**, 3597–3603 (1965). https://doi.org/10.1063/1.1696526

Terenzi, C., Sederman, A.J., Mantle, M.D., Gladden, L.F.: Enabling high spectral resolution of liquid mixtures in porous media by antidiagonal projections of two-dimensional 1 H NMR COSY spectra. J. Phys. Chem. Lett. **10**, 5781–5785 (2019). https://doi.org/10.1021/acs.jpclett.9b02334

Torrey, H.C.: Bloch equations with diffusion terms. Phys. Rev. **104**, 563–565 (1956). https://doi.org/10.1103/PhysRev.104.563

Wakao, N., Funazkri, T.: Effect of fluid dispersion coefficients on particle-to-fluid mass transfer coefficients in packed beds. Chem. Eng. Sci. **33**, 1375–1384 (1978). https://doi.org/10.1016/0009-2509(78)85120-3

Weber, D., Mitchell, J., McGregor, J., Gladden, L.F.: Comparing strengths of surface interactions for reactants and solvents in porous catalysts using two-dimensional nmr relaxation correlations. J. Phys. Chem. C **113**, 6610–6615 (2009). https://doi.org/10.1021/jp811246j

Yan, P., Marica, F., Guo, J., Balcom, B.J.: Direct measurement of pore size and surface relaxivity with magnetic resonance at variable temperature. Phys. Rev. Appl. **20**, 014009 (2023). https://doi.org/10.1103/PhysRevApplied.20.014009

Ye, S., Hou, Y., Li, X., Jiao, K., Du, Q.: Pore-scale investigation of coupled two-phase and reactive transport in the cathode electrode of proton exchange membrane fuel cells. Trans. Tianjin Univ. (2022). https://doi.org/10.1007/s12209-021-00309-4